J|A|C|S COMMUNICATIONS

Published on Web 02/13/2009

Synthesis of Titania Nanosheets with a High Percentage of Exposed (001) Facets and Related Photocatalytic Properties

Xiguang Han, Qin Kuang,* Mingshang Jin, Zhaoxiong Xie,* and Lansun Zheng

State Key Laboratory for Physical Chemistry of Solid Surfaces and Department of Chemistry, College of Chemistry and Chemical Engineering, Xiamen University, Xiamen 361005, China

Received November 26, 2008; E-mail: qkuang@xmu.edu.cn; zxxie@xmu.edu.cn

Over the past decades, surface chemists have made great achievements in the study of chemical properties of definite crystal planes by employing bulk single crystals.[1] However, it is difficult to directly apply single crystals in many technical fields, such as real catalysis. It is therefore necessary to set up a bridge between the surface chemistry of bulk single crystals and the real technical fields. The surface-controlled growth of micro- and nanocrystallites could be such a bridge.[2] TiO_2, as a wide-band-gap semiconducting material, is expected to play an important role in helping to ease the environmental and energy crisis through effective utilization of solar energy derived from photocatalysis, photovoltaics, and water photocatalysis.[3] Surface scientists have demonstrated that the order of the average surface energies of anatase TiO_2 is 0.90 J/m^2 for {001} > 0.53 J/m^2 for {100} > 0.44 J/m^2 for {101}.[4] Although it can be expected that the higher-surface-energy (001) surface has much higher chemical activities, almost all of anatase TiO_2 nanostructures reported to date have had low-energy (101) surfaces (few have had {100} facets).[5] Important progress was made very recently by Lu and co-workers,[6] who reported the synthesis of micron-sized anatase TiO_2 crystallites with highly energetic (001) facets exposed. However, the percentage of exposed (001) facets was only 47%, and the crystallite size was relatively large. In this communication, we report a facile hydrothermal route for synthesizing sheet-like anatase TiO_2 with the highly reactive (001) facets exposed that takes advantage of a specific stabilization effect of fluorine ions on the (001) facets. Excitingly, the percentage of highly reactive (001) facets in such TiO_2 nanosheets is very high (up to 89%). In addition, the as-prepared TiO_2 nanosheets exhibit excellent activity in the photocatalytic degradation of organic contaminants.

Sheet-like anatase TiO_2 was synthesized via a simple hydrothermal route using tetrabutyl titanate, $Ti(OBu)_4$, as a source and 47% hydrofluoric acid solution as the solvent (see the Supporting Information for experimental details). ***Caution!*** *Hydrofluoric acid is extremely corrosive and a contact poison, and it should be handled with extreme care.* Figure 1A showed a typical X-ray diffraction (XRD) pattern (PANalytical X-Pert) of TiO_2 nanosheets synthesized at 180 °C. The diffraction peaks could be indexed to anatase-phase TiO_2 (JCPDS No. 21-1272), indicating that the as-synthesized product was pure anatase TiO_2. Transmission electron microscopy (TEM) analysis (JEM-2100) showed that the product consisted of well-defined sheet-shaped structures having a rectangular outline, side length of ~40 nm, and thickness of ~6 nm (Figure 1B). A high-magnification TEM image and its corresponding selected-area electron diffraction (SAED) pattern (indexed as the [001] zone axis diffraction) indicated that the top and bottom facets of the nanosheets were the (001) planes, as shown in Figure 1C. The high-resolution TEM image (Figure 1D) directly showed that the lattice spacing parallel to the top and bottom facets was ~0.235 nm, corresponding to the (001) planes of anatase TiO_2. On the basis of the above structural information, the percentage of highly reactive (001) facets in the TiO_2 nanosheets shown in Figure 1 was estimated to be ~77%.

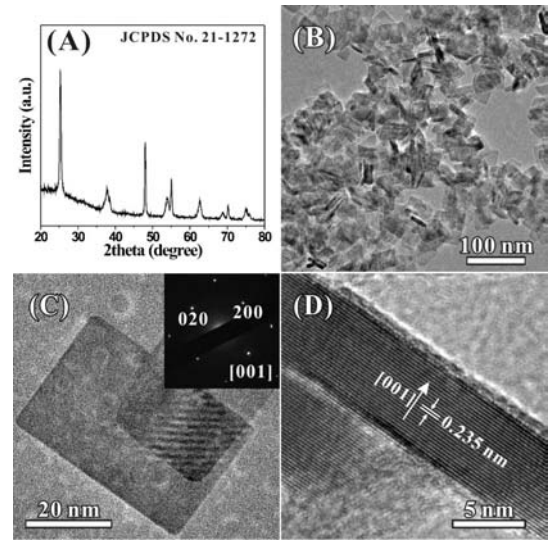

Figure 1. (A) Typical XRD pattern and (B) low-magnification TEM image of TiO_2 nanosheets synthesized at 180 °C using 5 mL of $Ti(OBu)_4$ and 0.6 mL of HF. (C) High-magnification TEM image of an individual TiO_2 nanosheet; the inset shows the corresponding SAED pattern. (D) High-resolution TEM image from the vertical nanosheets.

First-principles calculations indicate that fluorine ions can markedly reduce the surface energy of the (001) surface to a level lower than that of {101} surfaces.[6] As a result, the fluorine ions may play a key role in the formation of the exposed (001) surface, and a series of experiments was carried out by introducing different amounts of fluorine ions. When the volume of hydrofluoric acid was increased from 0.6 to 0.8 mL, the TiO_2 nanosheets became larger (~50 nm) (Figure 2A,B). The percentage of (001) facets in the sheets is surprisingly as high as ~80%. On the contrary, decreasing the volume of hydrofluoric acid resulted in a decrease in the size of the nanosheets (see Table S1 in the Supporting Information). Furthermore, the reaction temperature was also found to play a key role in controlling the thickness and size of the TiO_2 nanosheets. When the reaction temperature was raised, the TiO_2 nanosheets became larger and slightly thicker (Figure 2C,D). The optimum reaction conditions to give the maximum percentage of (001) facets were 200 °C, 5 mL of $Ti(OBu)_4$, and 0.8 mL of hydrofluoric acid. The average size of the as-prepared nanosheets reached 130 nm with a thickness of ~8 nm, and the average percentage of the (001) facets was as high as 89% (Figure 2D). All of the structural information [i.e., size, thickness, and percentage of (001) facets] for TiO_2 nanosheets synthesized under different reaction conditions are listed in Table S1 in the Supporting Information for comparison.

10.1021/ja8092373 CCC: $40.75

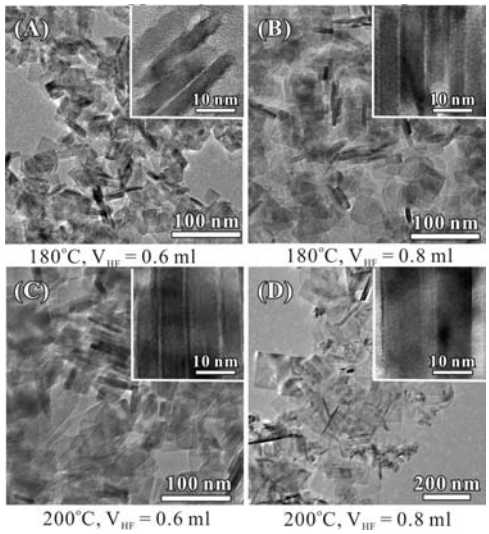

Figure 2. TEM images of TiO_2 nanosheets synthesized at (A) 180 °C, 5 mL of $Ti(OBu)_4$, and 0.6 mL of hydrofluoric acid; (B) 180 °C, 5 mL of $Ti(OBu)_4$, and 0.8 mL of hydrofluoric acid; (C) 200 °C, 5 mL of $Ti(OBu)_4$, and 0.6 mL of hydrofluoric acid; and (D) 200 °C, 5 mL of $Ti(OBu)_4$, and 0.8 mL of hydrofluoric acid. The insets show corresponding transmission electron microscopy images of vertical TiO_2 nanosheets that show the thickness of the nanosheets.

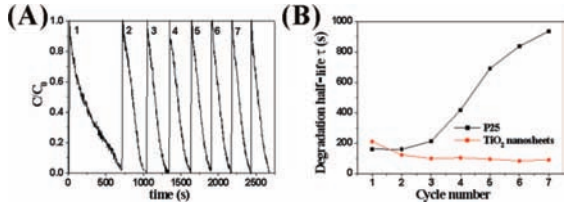

Figure 3. (A) Cycling degradation curve for TiO_2 nanosheets [89% (001) facets] synthesized under the optimum reaction conditions, using 1 mmol/L MO as a probe. (B) Degradation half-life of MO for as-synthesized TiO_2 nanosheets and commercial P25 as a function of cycle number. The vertical axis here shows the degradation half-life of MO, i.e., the time required for half of the MO molecules to degrade.

The as-synthesized TiO_2 nanosheets surrounded by (001) facets are expected to exhibit high photocatalytic efficiency. In our experiments, methyl orange (MO) was used as a probe molecule to investigate the photocatalytic performance. Furthermore, commercially available Degussa P25 TiO_2 (average particle size of 25 nm) was used as a reference for comparison (Figure S1 in the Supporting Information). It was found that the as-prepared TiO_2 nanosheets exhibited a gradually accelerating degradation rate (Figure 3A,B) and that the degradation efficiency was higher than that of P25 TiO_2 after the first degradation cycle. Furthermore, TiO_2 nanosheets with a higher percentage of (001) facets exhibited more effective photocatalytic performance (Figure S2 in the Supporting Information), demonstrating the high catalytic activity of the (001) facets.

Interestingly, the degradation rate for the as-prepared nanosheets was relatively small during the first cycle. The abnormal performance of the TiO_2 nanosheets in the first cycle could be due to the presence of superficial inorganic species and organic adsorbates on the TiO_2 nanosheets at the beginning. After the first cycle, the inorganic species were desorbed from the surface and the organic adsorbates degraded, resulting in the accelerating degradation rate in the following degradation cycles. This hypothesis was also certified by directly cleaning the TiO_2 nanosheets with 0.1 M NaOH, during which the adsorbed fluorine ions on the surface of TiO_2 are easily replaced by hydroxyl groups.[7] The degradation efficiency of the TiO_2 nanosheets after cleaning with alkaline solution was found to be remarkably improved, as shown in Figure S3 in the Supporting Information. As for the P25, conversely, the degradation rates gradually decreased after three degradation cycles, possibly because of adsorption of incompletely photodecomposed products on the surface of the P25.

In conclusion, rectanglar TiO_2 nanosheets with highly reactive (001) facets as the top and bottom surfaces have been successfully synthesized by a simple hydrothermal route with the assistance of hydrofluoric acid solution. The percentage of (001) facets in the sheets was 89% with the optimal adjustment of the amount of hydrofluoric acid and reaction temperature. Such TiO_2 nanosheets show excellent photocatalytic efficiency, far exceeding that of commercially available Degussa P25, due to exposure of the high percentage of (001) facets. The present study motivates us to further explore the hydrothermal synthetic method for the preparation of other metallic oxides with a high percentage of reactive facets, which have promising applications as gas sensors, photocatalysts, solar cells, and photonic and optoelectronic devices.

Acknowledgment. This work was supported by the National Natural Science Foundation of China (Grants 20725310, 20721001, 20673085, and 20801045) and the National Basic Research Program of China (Grants 2007CB815303 and 2009CB939804).

Supporting Information Available: Experimental details, structural information for TiO_2 nanosheets synthesized under different reaction conditions, cycling degradation curves for commercial P25 and TiO_2 nanosheets with different percentages of (001) facets, and degradation curves of TiO_2 nanosheets with and without the 0.1 M NaOH washing treatment. This material is available free of charge via the Internet at http://pubs.acs.org.

References

(1) (a) Kiskinova, M. *Chem. Rev.* **1996**, *96*, 1431. (b) Somorjai, G. A. *Chem. Rev.* **1996**, *96*, 1223. (c) Seker, F.; Meeker, K.; Kuech, T. F.; Ellis, A. B. *Chem. Rev.* **2000**, *100*, 2505.
(2) (a) Tian, N.; Zhou, Z. Y.; Sun, S. G.; Ding, Y.; Wang, Z. L. *Science* **2007**, *316*, 732. (b) Fan, D.; Thomas, P. J.; O'Brien, P. *J. Am. Chem. Soc.* **2008**, *130*, 10892. (c) Liao, H. G.; Jiang, Y. X.; Zhou, Z. Y.; Chen, S. P.; Sun, S. G. *Angew. Chem., Int. Ed.* **2008**, *47*, 9100. (d) Zhou, X.; Xie, Z. X.; Jiang, Z. Y.; Kuang, Q.; Zhang, S. H.; Xu, T.; Huang, R. B.; Zheng, L. S. *Chem. Commun.* **2005**, 5572. (e) Ma, Y. Y.; Kuang, Q.; Jiang, Z. Y.; Xie, Z. X.; Huang, R. B.; Zheng, L. S. *Angew. Chem., Int. Ed.* **2008**, *47*, 8969.
(3) (a) Chen, X. B.; Mao, S. S. *Chem. Rev.* **2007**, *107*, 2891. (b) Joo, J.; Kwon, S. G.; Yu, T.; Cho, M.; Lee, J.; Yoon, J.; Hyeon, T. *J. Phys. Chem. B* **2005**, *109*, 15297. (c) Wijnhoven, J. G. J.; Vos, W. L. *Science* **1998**, *281*, 802. (d) Barbe, C. J.; Arendse, F.; Comte, P.; Jirousck, M.; Lenzmann, F.; Shklover, V.; Gratzel, M. *J. Am. Ceram. Soc.* **1997**, *12*, 3157. (e) Tang, J. W.; Durrant, J. R.; Klug, D. R. *J. Am. Chem. Soc.* **2008**, *130*, 13885. (f) Park, H.; Vecitis, C. D.; Choi, W.; Weres, O.; Hoffman, M. R. *J. Phys. Chem. C* **2008**, *112*, 885.
(4) (a) Lazzeri, M.; Vittadini, A.; Selloni, A. *Phys. Rev. B* **2002**, *65*, 119901. (b) Diebold, U. *Surf. Sci. Rep.* **2003**, *48*, 53.
(5) (a) Zhang, Z. H.; Zhong, X. H.; Liu, S. H.; Li, D. F.; Han, M. Y. *Angew. Chem., Int. Ed.* **2005**, *44*, 3466. (b) Buonsanti, R.; Grillo, V.; Carlino, E.; Giannini, C.; Kipp, T.; Cingolani, R.; Cozzoli, D. *J. Am. Chem. Soc.* **2008**, *130*, 11223. (c) Seo, J. W.; Jun, Y. W.; Ko, S. J.; Cheon, J. W. *J. Phys. Chem. B* **2005**, *109*, 5389. (d) Wen, P. H.; Itoh, H.; Tang, W. P.; Feng, Q. *Langmuir* **2007**, *23*, 11782. (e) Wu, B. H.; Guo, G. Y.; Zheng, N. F.; Xie, Z. X.; Stucky, G. D. *J. Am. Chem. Soc.* **2008**, *130*, 17563.
(6) Yang, H. G.; Sun, C. H.; Qiao, S. Z.; Zou, J.; Liu, G.; Smith, S. C.; Cheng, H. M.; Lu, G. Q. *Nature* **2008**, *453*, 638.
(7) Wang, Q.; Chen, C. C.; Zhao, D.; Ma, W. H.; Zhao, J. C. *Langmuir* **2008**, *24*, 7338.

JA8092373